# Supplementary Material

## 1 EXTINCTION HYPOTHESES

Several hypotheses have been put forward regarding the extinction of *H. damalis*. It is certain that pre-industrial hunting is responsible for the death of the last individuals, but the single known population was geographically restricted, and may have numbered as few as 2,000 individuals (Sharko et al., 2021). Recent reconstruction of a *H. damalis* genome points to a population bottleneck suffered roughly 400,000 years ago. Coupling the subsequent reduction of genetic diversity with presumed population fragmentation during intervals of glacially-lowered sea level, Sharko et al. (2021) suggested that the species was doomed to extinction prior to historical exploitation, a type of "dead clade walking" (Jablonski, 2001). There are arguments that the lowering of sea level during intervals of glacial expansion would have reduced the shallow coastal habitat required by giant kelp, and the Comander Islands population was therefore a relict one. The Comander Islands, however, are not the likeliest location for a glacial refuge in the North Pacific, because of the limited benthic shelf area that would be available for giant kelp forests. Significantly more habitat space would have been available in the Bering Sea and off southeast Alaska.

It remains possible though that the Comander Islands population was itself the remnant of a recent expansion following the last glacial termination approximately 10,000 years ago. Graham et al. (2010) have argued for a threefold expansion of *M. pyrifera* forests in southern California between the last glacial maximum and the mid-Holocene, followed by a rapid decline. This type of response probably also occurred further to the north (Graham et al., 2010), although the timing may have differed. In that case, the historical population of the Comander Islands may indeed have been a geographic relict, but the ability of the species to undergo range expansions and contractions, and to persist through multiple glacial-interglacial cycles, would refute the hypothesis that this was a clade pre-destined for extinction. Our argument is supported by the discovery of *H. gigas* bones from St. Lawrence Island to the north in the Bering Sea, dated to 800-920 CE.

Hunting by regional Indigenous peoples has also been proposed as a cause of the species' limited range by historical times, although there is no archaeological evidence to support this. Crerar et al. (2014) suggested that Inuit, expanding into the Bering Sea during the Medieval Warm Period (950-1250 CE), may have hunted the species, basing this on the coincidental occurrence of Inuit migration with the St. Lawrence Island specimen, but there are no records of hunting, and no remains of *H. gigas* have to-date been associated with the activities of Indigenous peoples.

Finally, it has been proposed that the small population size and geographic restriction documented by Steller were secondary consequences of a widespread transition of giant kelp forests to urchin barrens caused by Indigenous and Russian over-exploitation of sea otters (Haley, 1980; Anderson, 1995; Anderson and Domning, 2009). There is no evidence that Indigenous peoples over-exploited sea otters to the extent that kelp forests underwent state transitions, although it has been suggested that sustainable use and management limited local population sizes Pinkerton et al. (2019). Whether they could have driven population declines or extirpation of *H. gigas* is an open question. What is entirely plausible is that *H. gigas*, like many other Pleistocene-Holocene mammalian megafaunal species may have been vulnerable to the interval's significant climatic fluctuations, and thus to the combined climate change and prehistoric hunting proposed for terrestrial scenarios in the Americas and Australia (Martin et al., 1984; Barnosky and Lindsey, 2010; Saltré et al., 2019). Population modeling of *H. gigas* by Turvey and Risley (2006) supports the

contention that small bands of pre-industrial hunters could have been a sole cause of extirpation, but that the documented intensity of $18^{\mathtt{th}}$ century hunting suggests that the Comander Island population was actually larger than indicated in written accounts. Therefore the only certainty is that the last known individuals of Steller's sea cow were killed and consumed by Russia-based commercial venturers.

## 2 SUPPLEMENTARY METHODS

There is a considerable number of biological parameters in the model system. Some parameter values are derived empirically, for example, the dependence of sea urchin exposure on population size and macroalgal densities. A number of parameter values, however, although being in the range of what may be considered reasonable based on ecological knowledge, were tuned here to accomplish feasibility of unperturbed models. Examples include intrinsic rates of increase of algal species, and mortality rates of consumers. It is important to understand the sensitivity of model behaviour to these assumptions. We therefore conducted sensitivity analyses of several parameters (Supplemental Material). We did not conduct a global sensitivity analysis, where one performs an exhaustive exploration of all parameter combinations, as the number of such combinations is computationally prohibitive. We instead conducted a series of tests of local sensitivity, considering sets of related parameters.

Formulae in the following sections are short-handed in two ways. First, many variables are time-dependent, but in our differential equations we shorten $x(t)$ to simply $x$ to maintain readability of the formulae. Second, variables that denote similar processes or interactions, such as predator-prey functions should be subscripted to identify the specific interactions that they represents, e.g. $\omega_{UW}$ vs. $\omega_{PU}$, indicating sea urchin herbivory of kelp and sea star predation of urchins respectively. Again, to maintain readability of long formulae, we subscript such variables numerically, e.g. $\omega_1$ and $\omega_4$. Table 1 lists precise definitions of all parameters and variables.

### 2.1 Physical parameters

Three physical parameters are present in the models: seasonal day length, which controls kelp and understory algal productivity; wave energy, which creates the probability that adult kelp will be dislodged and removed from the population; and sea surface temperature, which seasonally affects the metabolic rates and therefore ecological parameters of kelp, understory algae, and invertebrates.

#### 2.1.1 Temperature

A core tenet of the Metabolic Theory of Ecology (MTE) is that environmental temperature affects the basal cellular metabolic rates of many organisms (Brown et al., 2004), and as a consequence, the efficiency of energy assimilation and intrinsic rates of increase ("$r$") of species populations. For example, a typical relationship exists between maximum $r$, designated here as $r_{\mathtt{max}}$, at a species-specific optimum temperature $T_{\mathtt{opt}}$ (other physical factors being held constant). $r$ declines slowly below $T_{\mathtt{opt}}$, often remaining positive down to 0°C for organisms in cool temperate and polar waters (Hurford et al., 2019). In contrast, $r$ may decline sharply above $T_{\mathtt{opt}}$, approaching zero between 20-25°C for those same organisms. Empirical determinations of the sea surface temperature (SST)-$r$ relationship are few, but resemble inverted skewed parabolas and are generally fit with a Sharpe-Schoofield model (Schoolfield et al., 1981). Here we model the relationships using a Linex loss function (Chang and Hung, 2007), which bears a similar geometric form. For example, the dependence of species-specific $r$ on temperature is described as

$$r = \frac{r_{\mathtt{max}}}{1.5}\left(4 + x - e^{x}\right) \tag{S1}$$

where

$$x = 2\left[\frac{T - 3.7}{T_{\mathtt{opt}}} - 1.5\right] \tag{S2}$$

The choice of this function is *ad hoc*, but it captures the essential morphology of the relationship (Fig. S1A), including positivity at 0°C, a maximum $r$ at $T_{\mathtt{opt}}$, and an intercept of the SST axis at $\approx$ 25°C. $T_{\mathtt{opt}}$ itself is determined either from empirical studies of the model system's species, or from the maximum seasonal temperature of the mid-point of the geographic range of a species for which the value is unmeasured. The occurrences and densities of both *S. purpuratus* and *P. helianthoides* have been shown to be temperature-dependent, with *S. purpuratus* being increasingly common at temperatures exceeding 14°C and *P. helianthoides* less common (Bonaviri et al., 2017). Model optimal temperatures are listed in Table 1 for *M. pyrifera*, *C. corymbiferus*, *S. purpuratus* and *P. helianthoides*.

Sea surface temperature itself is calculated as

$$T = 14.64 + \left[2.2\cos\left(2\pi\frac{D - 233}{365}\right)\right] \tag{S3}$$

where $D$ is the numerical day of the year, and 14.64$^o$C is the mean annual SST of Monterey Bay, California (Monterey Bay National Marine Sanctuary) (Fig. S1B). This function has a low frequency, multi-decadal scale variation that captures decadal variation in the North Pacific, though this is not relevant for the sub-decadal perturbations considered in this study.

### 2.1.2 Day length

Day length $\Delta d$ is the number of hours per day for which light intensity is above the minimum threshold required for photosynthesis ($\approx$1%). It varies latitudinally and seasonally. Annual daylength is calculated for Monterey Bay based on a maximum of 14.67 hours of daylight and a minimum of 9.67 hours, as

$$\Delta d = \left[2.5\cos\left[0.017\left(D - 172\right)\right]\right] + 12.67 \tag{S4}$$

where $D$ is the numerical day of the year (Fig. S1C).

### 2.1.3 Hydrodynamic forces

On the central California coast today, the major source of kelp mortality in the forested state is dislodgement by hydrodynamic forces. Kelp can withstand substantial drag because of their flexibility, and the attenuation of wave energy by the density of the forest itself. Nevertheless, high energy waves and storm surges are capable of dislodging giant kelp. Most of this mortality occurs in late winter, when up to 90% of adult individuals in a single forest can be removed (Foster et al., 2015). This process is likely very important to the community's dynamics as it both provides a mechanism for persistence of understory algae, as well as creates a decline of the drift detritus supply.

We modeled storm occurrence and associated wave height based on sub-daily wave height measures in Monterey Bay for the years 2009-2020 (National Oceanographic and Atmospheric Administration, Monterey Bay Aquarium historical sensor data, Buoy Station - sea_surface_wave_significant_height). The model simplifies the fact that any single event of extreme wave height is likely to have an autocorrelation length of several days, where the occurrence of extreme waves is distributed over several consecutive days. This means that a cumulative total of $n$ kelp plants are removed during that entire interval, not $n$ plants per day. Combining multiple years of data can exacerbate this effect by increasing the possible duration of

events because they occur at approximately the same times of year, but not exactly on the same days. Storm surge events were therefore sampled from a modeled smooth cosine function that captures, at maximum amplification, the wave height threshold above which adult kelp become susceptible to removal. To this function is added an uncorrelated daily noise, tuned low enough to allow persistence of the biotic system (Fig. S1D).

Wave height was therefore modeled as a wave that has its maximum amplitude at 2.5 m, to which is added a noise sufficient to capture stochastically extreme wave heights sufficient to dislodge kelp.

$$w = \eta_1 - \left\{1.5 + \left[\frac{1}{2}\cos\left[2\pi\left(\frac{D-233}{365}\right)\right]\right] + 3.5\right\} \tag{S5}$$

where $w$ is wave height (meters) and $\eta_1$ is a random noise ranging $[-0.1, 0.1]$. Furthermore, $\delta_M$, the surge-driven mortality rate of adult kelp, is given as

$$\delta_M = \begin{cases} 0.0001 + \eta_2 & \texttt{if } w > 2.5, \texttt{and} \\ 0 & \texttt{if } w \leq 2.5 \end{cases} \tag{S6}$$

where $\eta_2$ is a random noise ranging $(0, 0.000075]$."

### 2.1.4 Species dynamics and biotic interactions

#### *2.1.4.1 Kelp*

The intrinsic rate of increase is a daily rate, and should be imagined as a reasonable number of replacements when integrated over a year. For example, $r = 0.05$ would result in a replacement of one adult kelp by $\approx 384$ individuals, if growth was uninhibited and exponential. That value is modified by setting $T_{\texttt{opt}} = 15$°C. A mean canopy frond density of 20 fronds per individual adult is assumed based on empirical surveys (Van Tussenbroek, 1993). It is further assumed in the model that kelp and understory algae are equal or neutral competitors for space on the substrate. Therefore maximum kelp density could increase twofold in the absence of spatial understory competitors. Therefore, if the dependence of the intrinsic rate of increase on temperature and day length is formulated as

$$r = r_{\texttt{T}}\left[1 - (0.1\Delta D)\right] \tag{S7}$$

where $r_{\texttt{T}}$ (T = sea surface temperature) is calculated according to Equation S1 (Supplementary Material) and day length $\Delta D$ is less than 10 hours, then the population will grow logistically in the absence of predation.

$$\frac{dM}{dt} = \frac{rMF}{20}\left(1 - \frac{M}{2-C}\right) \tag{S8}$$

where $M$ is kelp density, $F$ is frond density and $C$ is the density of understory algae.

Urchin browsing of adult kelp is represented as

$$M(U_E\omega_1) \tag{S9}$$

where $U_E$ is the proportion of the urchin population comprising mobile, active foragers (in contrast to sheltered detritivores), and $\omega_1$ is a predator-prey interaction. $\omega_1$ is a functional interaction between urchins and kelp, meaning that the interaction itself is dynamic, changing with prey and predator densities.

Here we use an Arditi-Ginzburg-Contois (AGC) function (Arditi and Ginzburg, 2012), which recognizes prey:predator ratio and predator density as controlling factors in the interaction.

$$\omega_1 = \frac{\alpha_1 U_E M}{U_E + \alpha_1 M} \tag{S10}$$

where $\alpha_1$ is the interaction strength between prey and predator.

Local kelp extinction is offset by external recruitment of kelp larvae, which is additional to reproduction by community members. As with the intrinsic rate of increase, the success of recruits is dependent on water temperature, successful settlement and growth, and hence the density of canopy fronds and the amount of light that reaches the benthos. This term is expressed as

$$\sigma_M(T)\left(1 - \frac{M + C}{2}\right)(1 - 0.03F) \tag{S11}$$

where $\sigma_M(T)$ (from hereon simply $\sigma_M$) is the temperature-dependent external recruitment rate, $M$ and $C$ are the densities of kelp and understory algae, respectively, which dominate the space available for settlement, and $0.03F$ is light availability. Note that the limiting terms based on kelp and understory algal densities ($M$ and $C$) are not symmetric for adult kelp and externally recruited juveniles. The former are limited only by spatial competition, whereas the latter are limited by both spatial competition, as well as shading by adult kelp. The recruitment rate itself is temperature-dependent, expressed as

$$\sigma_M = \frac{\sigma_M}{1.5}\left[4 + 2\left(\frac{\mathtt{T} - 3.7}{15} - 1.5\right)\right] - e^x \tag{S12}$$

where

$$x = \frac{\mathtt{T} - 3.7}{15} - 1.5 \tag{S13}$$

This is a Linex function as in Eq. S1.

Note that Eq. 1 (main text) has a discontinuity when $C = 2$; that is, the substrate is completely taken over by understory algae. This is a mathematical aberration only, as the situation implies trivially that the kelp population is then zero, and cannot rise above zero unless new kelp are recruited, and space on the substrate is made available somehow.

#### *2.1.4.2 Sea urchins*

Two common species of strongylocentrotid urchins exist in kelp forests of the Pacific northwest: *Strongylocentrotus purpuratus* and *Mesocentrotus franciscanus*, the purple and red sea urchins, respectively. Both are treated as a single unit in the model, but in reality, although the two species are associated with the transition between forested and barren system states, the purple urchin is by far the dominant species in barrens in California.

The major controls of sea urchin dynamics are population density and food supply. Urchins prefer to remain sedentary and sheltered from predation using the topography of the benthic substrate. When sheltered and sedentary, urchins feed primarily on drifting algal detritus. All such detritus in the model is produced by *M. pyrifera* and *C. corymbiferus* (Eq. 3 in main text). Nevertheless, a small fraction of the population can usually be found exposed and mobile even when detrital production is high (Smith et al., 2021). Mobile urchins consume both detritus and living algae, and are responsible for the transition from

the forest to the barrens state. The proportion of the urchin population that is actively foraging increases as population density increases, possibly because of crowding in the substrate. It also grows if detrital concentration declines (Harrold and Reed, 1985), and competition within the sedentary lifestyle increases. There is thus a positive feedback between active foraging and the necessity of leaving crevices.

The proportion of exposed urchins, $U_E$, is modeled as follows. First it is assumed that there is a finite amount of space available in the substrate for sheltering urchins. Using data available for Monterey Bay, California (Smith et al., 2021), we estimated that if total urchin density is less than the amount of available space, then the proportion of exposed urchins, that is, mobile foragers, may be estimated as

$$U_E = 0.22 \ln(U) \tag{S14}$$

($r^2 = 0.45$, $p < 0.0001$). There is also a weaker dependency on kelp density, as indicated by the gonadal condition (gonad index) of the urchins. We assumed detrital density to be a direct function of adult urchin density, and that near the carrying capacity of sheltered urchins the proportion of exposed urchins is approximately 0.35 (Smith et al., 2021). Thus, we modeled the relationship between exposed urchins, total urchin density and available drift detritus as

$$U_E = 0.22 \ln(U) - 0.08 \ln(G) + 0.0018[\ln(U) \ln(G)] + 0.35 \tag{S15}$$

(multiple least squares regression; $R^2 = 0.45$, p<0.0001) where $U$ is total urchin density and $G$ is detrital density (Fig. S3).

## 2.2 Probability of sea otter presence

Sea otters (*Enhydris lutris*) are present in a community only when sea urchins (*Strongylocentrotus purpuratus*) are of sufficient nutritive value. That value declines as a function of declining kelp and other edible algal densities, and is typically measured as gonadal index, which is the fraction of body weight accounted for by gonadal tissues. Smith et al. (Smith et al., 2021) related the frequency of sea otter site selection for predation to gonadal index. From their data (their Fig. 4) we estimated the following relationship between the probability of otter predation and gonadal index

$$p(\texttt{otters}) = \frac{0.934}{1 + \texttt{exp}(-0.206(\texttt{GI} - 11.31))} \tag{S16}$$

where GI is gonadal index. GI in turn is derived by inverting the relationship between it and the fraction of the urchin population that is exposed (given by text Equation 17),

$$\texttt{GI} = -5x + 7 \tag{S17}$$

## 2.3 Model parameterization

Model parameters were determined using a combination of both empirical and theoretical relationships among organismal traits and external variables, and a criterion of system feasibility; that is, all species persist and co-exist in an unperturbed community and none become extinct during the burn-in interval. A complete list is given in Table 1. Most parameter values were invariable among models and simulations, but several were drawn stochastically from distributions to reflect real-world uncertainty and variability of their values. The latter include: wave height; the presence of sea otters as urchin predators; rates of intrinsic

increase of the algae *M. pyrifera* and *C. corymbiferus*; consumer mortality rates; and ecological efficiencies of the consumers *S. purpuratus*, *P. helianthoides* and *H. gigas*.

### 2.3.1 Rates of intrinsic increase

Rates of intrinsic increase of *M. pyrifera* and *C. corymbiferus* were set at $0.1 \pm \lambda$, where $\lambda$ is drawn randomly from a normal distribution of mean zero and standard deviation 0.025 ($\mathcal{N}(0, 0.025)$).

### 2.3.2 Algal recruitment rates

Rates of recruitment of *M. pyrifera* and *C. corymbiferus* were assumed to be $0.001\mathtt{d}^{-1}$ and $0.0001\mathtt{d}^{-1}$ respectively. These rates are derived from those presented by Detmer et al. (2021), but modified to maintain feasibility of the populations under the conditions of both spatial competition and predation in the current model.

### 2.3.3 Kelp frond senescence

Kelp fronds eventually decline in photosynthetic activity and detach from the main stipe, becoming part of the pool of drift detritus. They do this in the model at a rate of $0.0125\mathtt{d}^{-1}$ (Detmer et al., 2021).

### 2.3.4 Rates of mortality

Mortality rates of the consumers (otters excepted as their demographics are not controlled by model interactions) were estimated based on empirical scaling relationships between measured mortality rates and body masses for a wide range of organisms (McCoy and Gillooly, 2008). The relationship was further scaled to yield feasibility of more than 90% of unperturbed models, as determined by 100 simulations per model type (Historical and Modern, with and without otters). The relationship is

$$\delta = \frac{xe^{-0.25m-1.06}}{365} \tag{S18}$$

where $\delta$ is a daily mortality rate, $m$ is body mass (grams), and $x$ =300 for *S. purpuratus* and 30 for *P. helianthoides* and *H. gigas*.

### 2.3.5 Ecological efficiency

Ecological efficiency, $\varepsilon$, is the rate or efficiency with which consumed prey are converted into new predators. Estimates vary widely in theoretical models, but are often assumed to be 0.1. This value is justified as the thermodynamic "rule of thumb" of an ≈10% efficiency of energy assimilated from consumed organic material. That value is used here for sea urchin, sunflower sea star and sea cow efficiencies, but to each value of 0.1 per simulation is added a small stochastic variation drawn from a normal distribution, $\mathcal{N}$(0.0,0.003).

### 2.3.6 Otter predation

The probability that otters are present and preying on *S. purpuratus* was derived from an empirical study of otter predation and urchin nutritive condition as measured using gonadal index (Smith et al., 2021). Because urchin condition is a function of kelp density, we related otter activity directly to kelp density (text Eq. 17). We rendered the relationship probabilistic by having otters present if $E < p$, where $p$ is generated randomly from a uniform distribution.

# 3 SENSITIVITY ANALYSES

## 3.1 Intrinsic rates of increase

Rates of intrinsic increase of the algae *M. pyrifera* and *C. corymbiferus* are set at 0.1 day$^{-1}$ (Supplemental Table 1) plus (minus) a stochastically determined variance, reflecting uncertainty of the true value. Model sensitivity was tested by generating the assumed mean values stochastically as $0.1 \pm \mathcal{N}(0.0, 0.01)$, representing deviations of the parameters by 10% or more from the assumed values. The tests were applied to the unperturbed Historical and Modern models, with and without sea otters, comparing the types and frequencies of different emergent states between the main simulations, and 100 altered simulations per model.

All sensitivity simulations generated the same types of states as those generated from the standard models, that is, stable kelp-dominated forests, both high and low diversity, as well as a metastable state in which systems oscillated quasiperiodically between forested and barren states. Furthermore, the frequencies did not differ significantly between the standard and altered models in any cases (Chi-square tests: Historical, $\chi^2 = 0.793, p = 0.373$; Historical without sea otters, $\chi^2 = 2.603, p = 0.107$; Modern, $\chi^2 = 2.863, p = 0.091$; Modern without sea otters, $\chi^2 = 0.883, p = 0.347$).

## 3.2 Mortality rates

Mortality rates for the consumers *S. purpuratus*, *P. helianthoides* and *H. gigas* were derived from a multi-taxon empirical relationship between body mass and mortality rate (see above). The formulae for each consumer (Eq. S8) were scaled by a species-specific factor, $x$, to maximize feasibility of the resulting system. We tested the sensitivity of this factor by increasing the variance of $x$ stochastically at levels of $0.01x$, $0.05x$ and $0.1x$ (Fig. S4), conducting 100 simulations per level per model type, and comparing the resulting state frequencies to the standard models and values of $x$.

Sensitivity varied among the models, with the Historical (with sea otters) and Modern (without sea otters) being insensitive to variation of $x$ up to 5% (Fig. S4, Table S7). The Historical model without sea otters, and the Modern model with sea otters, however, were more sensitive, deviating from the standard models at variance of $x$ greater than 1%. Nevertheless, all values of $x$ in the standard models may therefore vary while being consistent with results reported in the main text.

# REFERENCES

Anderson, P. K. (1995). Competition, predation, and the evolution and extinction of Steller's sea cow, *Hydrodamalis gigas*. Marine Mammal Science 11, 391–394

Anderson, P. K. and Domning, D. P. (2009). Steller's sea cow: *Hydrodamalis gigas*. In Encyclopedia of Marine Mammals (Elsevier). 1103–1106

Arditi, R. and Ginzburg, L. R. (2012). How species interact: altering the standard view on trophic ecology (Oxford University Press)

Barnosky, A. D. and Lindsey, E. L. (2010). Timing of Quaternary megafaunal extinction in South America in relation to human arrival and climate change. Quaternary International 217, 10–29

Bonaviri, C., Graham, M., Gianguzza, P., and Shears, N. T. (2017). Warmer temperatures reduce the influence of an important keystone predator. Journal of Animal Ecology 86, 490–500

Brown, J. H., Gillooly, J. F., Allen, A. P., Savage, V. M., and West, G. B. (2004). Toward a metabolic theory of ecology. Ecology 85, 1771–1789

Chang, Y.-c. and Hung, W.-l. (2007). LINEX loss functions with applications to determining the optimum process parameters. Quality & Quantity 41, 291–301

Crerar, L. D., Crerar, A. P., Domning, D. P., and Parsons, E. (2014). Rewriting the history of an extinction–was a population of Steller's sea cows (*Hydrodamalis gigas*) at St Lawrence Island also driven to extinction? Biology Letters 10, 20140878

Detmer, A. R., Miller, R. J., Reed, D. C., Bell, T. W., Stier, A. C., and Moeller, H. V. (2021). Variation in disturbance to a foundation species structures the dynamics of a benthic reef community. Ecology 102, e03304

Foster, M. C., Byrnes, J. E., and Reed, D. C. (2015). Effects of five southern California macroalgal diets on consumption, growth, and gonad weight, in the purple sea urchin *Strongylocentrotus purpuratus*. PeerJ 3, e719

Graham, M. H., Kinlan, B. P., and Grosberg, R. K. (2010). Post-glacial redistribution and shifts in productivity of giant kelp forests. Proceedings of the Royal Society B: Biological Sciences 277, 399–406

Haley, D. (1980). The great northern sea cow: Steller's gentle siren. In Oceans. vol. 13, 7–11

Harrold, C. and Reed, D. C. (1985). Food availability, sea urchin grazing, and kelp forest community structure. Ecology 66, 1160–1169

Hurford, A., Cobbold, C. A., and Molnár, P. K. (2019). Skewed temperature dependence affects range and abundance in a warming world. Proceedings of the Royal Society B 286, 20191157

Jablonski, D. (2001). Lessons from the past: evolutionary impacts of mass extinctions. Proceedings of the National Academy of Sciences 98, 5393–5398

Martin, P. S., Klein, R., et al. (1984). Prehistoric overkill: the global model. Quaternary extinctions: a prehistoric revolution , 354–403

McCoy, M. W. and Gillooly, J. F. (2008). Predicting natural mortality rates of plants and animals. Ecology letters 11, 710–716

Pinkerton, E., Salomon, A. K., and Dragon, F. (2019). Reconciling social justice and ecosystem-based management in the wake of a successful predator reintroduction. Canadian Journal of Fisheries and Aquatic Sciences 76, 1031–1039

Saltré, F., Chadoeuf, J., Peters, K. J., McDowell, M. C., Friedrich, T., Timmermann, A., et al. (2019). Climate-human interaction associated with southeast Australian megafauna extinction patterns. Nature communications 10, 1–9

Schoolfield, R. M., Sharpe, P., and Magnuson, C. E. (1981). Non-linear regression of biological temperature-dependent rate models based on absolute reaction-rate theory. Journal of theoretical biology 88, 719–731

Sharko, F. S., Boulygina, E. S., Tsygankova, S. V., Slobodova, N. V., Alekseev, D. A., Krasivskaya, A. A., et al. (2021). Steller's sea cow genome suggests this species began going extinct before the arrival of Paleolithic humans. Nature communications 12, 1–8

Smith, J. G., Tomoleoni, J., Staedler, M., Lyon, S., Fujii, J., and Tinker, M. T. (2021). Behavioral responses across a mosaic of ecosystem states restructure a sea otter–urchin trophic cascade. Proceedings of the National Academy of Sciences 118

Turvey, S. and Risley, C. (2006). Modelling the extinction of Steller's sea cow. Biology Letters 2, 94–97

Van Tussenbroek, B. (1993). Plant and frond dynamics of the giant kelp, *Macrocystis pyrifera*, forming a fringing zone in the Falkland Islands. European Journal of Phycology 28, 161–165

# 4 SUPPLEMENTARY TABLES AND FIGURES

## 4.1 Tables

# TABLES

**Table S1.** Variable and parameter definitions and values.

| Parameter | Definition | Value |
|---|---|---|
| $M$ | *M. pyrifera* density | |
| $F$ | *M. pyrifera* frond density | |
| $C$ | *C. corymbiferus* density | |
| $U$ | *S. purpuratus* density | |
| $U_E$ | Density of exposed *S. purpuratus* | |
| $P$ | *P. helianthoides* density | |
| $H$ | *H. gigas* density | |
| $E$ | *E. lutris* density | |
| $T$ | sea surface temperature | |
| $\omega_i$ | ratio-dependent predatory-prey interactions | |
| $\omega_1$ | *S. purpuratus* - *M. pyrifera* | |
| $\omega_2$ | *S. purpuratus* - *C. corymbiferus* | |
| $\omega_3$ | *S. purpuratus* - drift detritus | |
| $\omega_4$ | *P. helianthoides* - *S. purpuratus*= | |
| $\omega_5$ | *H. gigas* - *M. pyrifera* | |
| $r_{\texttt{max}}$ | Maximum rate of intrinsic increase of *M. pyrifera* and *C. corymbiferus* | 0.1 day$^{-1}$ |
| $T_{\texttt{opt}}$ | Temperature at which $r$, $\alpha$ or $\varepsilon$ is maximum for a species | |
| | *M. pyrifera* | 15$^o$C |
| | *C. corymbiferus* | 13$^o$C |
| | *S. purpuratus* | 16$^o$C |
| | *P. helianthoides* | 13$^o$C |
| $D$ | Numerical day of the year | 1-365 |
| $\eta_1$ | Random noise added to deterministic wave height, $w$ | $[-0.1, 0.1]$ |
| $\eta_2$ | Random noise added to wave-driven *M. pyrifera* mortality, $\delta_M$ | $(0, 0.000075]$ |
| $\sigma_M$, $\sigma_C$ | *M. pyrifera* and *C. corymbiferus* recruitment rates ($\sigma_M(T)$ & $\sigma_C(T)$) | 0.001 day$^{-1}$ |
| $\alpha_i$ | Predator-prey interaction coefficients ($\alpha_i(T)$) | |
| $\alpha_1$ | *S. purpuratus* - *M. pyrifera, C. corymbiferus* | 0.1 |
| $\alpha_2$ | *P. helianthoides* - *S. purpuratus* | 0.05 |
| $\alpha_3$ | *E. lutris* - *S. purpuratus* | 0.00005 |
| $\alpha_4$ | *H. gigas* - *M. pyrifera* fronds | 0.00002 |
| $\varepsilon_i$ | ecological efficiency ($\varepsilon_i(T)$) | |
| $\varepsilon_1$ | *S. purpuratus* | 0.1 |
| $\varepsilon_2$ | *P. helianthoides* | 0.1 |
| $\varepsilon_3$ | *H. gigas* | 0.1 |
| $\delta_F$ | *M. pyrifera* frond senescence rate | 0.0125 day$^{-1}$ |
| $\delta_i$ | Mortality rates | |
| $\delta_1$ | *S. purpuratus* | 0.0900 day$^{-1}$ |
| $\delta_2$ | *P. helianthoides* | 0.0034 day$^{-1}$ |
| $\delta_3$ | *H. gigas* | 0.00005 day$^{-1}$ |

**Table S2.** Correlation coefficients and probabilities of significance between population parameters and system state.

| Parameter | $r^2$ | p(significance level) |
|---|---|---|
| kelp $r$ | 0.0584 | 0.5639 |
| understory algal $r$ | 0.1372 | 0.1735 |
| sea urchin $\varepsilon$ | 0.7180 | $<$0.0001 |
| sunflower sea star $\varepsilon$ | 0.0792 | 0.4336 |

**Table S3.** Frequencies of transitions of forested state in response to perturbation. MHW - marine heat ave; SSWD - sea star wasting disease. Frequencies report the number of simulations out of 100 that transitioned to quasiperiodicity, were resistant to transition, or were resilient, instead transitioning temporarily to quasiperiodicity.

| Model | Perturbation | Quasiperiodic | Resistant | Resilient |
|---|---|---|---|---|
| Historical | MHW | 2 | 82 | 1 |
| | SSWD | 5 | 66 | 13 |
| | MHW+SSWD | 12 | 51 | 20 |
| Historical, no otters | MHW | 0 | 69 | 2 |
| | SSWD | 2 | 24 | 51 |
| | MHW+SSWD | 0 | 20 | 49 |
| Modern | MHW | 2 | 68 | 1 |
| | SSWD | 3 | 45 | 33 |
| | MHW+SSWD | 1 | 43 | 32 |
| Modern, no otters | MHW | 0 | 67 | 2 |
| | SSWD | 2 | 16 | 48 |
| | MHW+SSWD | 0 | 25 | 51 |

**Table S4.** Chi-square probabilities of differences of frequencies of resistant simulations between pairwise comparisons of model-perturbation combinations. See Table S1 for explanation of which models of each pair had the higher (lower) frequency.

| | Hw | Hd | Hwd | Hw_no | Hd_no | Hwd_no | Mw | Md | Mwd | Mw_no | Md_no | Mwd_no |
|---|---|---|---|---|---|---|---|---|---|---|---|---|
| Hw | | 0.0006 | 9E-06 | 0.4706 | 9E-06 | 9E-06 | 0.8952 | 9E-06 | 9E-06 | 0.4548 | 9E-06 | 9E-06 |
| Hd | | | 0.0838 | 0.0054 | 9E-06 | 9E-06 | 0.0019 | 0.0004 | 0.0003 | 0.0064 | 9E-06 | 9E-06 |
| Hwd | | | | 3E-05 | 9E-06 | 9E-06 | 9E-06 | 0.0718 | 0.0675 | 4E-05 | 9E-06 | 9E-06 |
| Hw_no | | | | | 9E-06 | 9E-06 | 0.5764 | 9E-06 | 9E-06 | 0.9769 | 9E-06 | 9E-06 |
| Hd_no | | | | | | 0.6948 | 9E-06 | 0.0014 | 0.0018 | 9E-06 | 0.3636 | 0.965 |
| Hwd_no | | | | | | | 9E-06 | 0.0005 | 0.0006 | 9E-06 | 0.6052 | 0.2582 |
| Mw | | | | | | | | 9E-06 | 9E-06 | 0.5594 | 9E-06 | 9E-06 |
| Md | | | | | | | | | 0.9642 | 9E-06 | 0.0009 | 0.002 |
| Mwd | | | | | | | | | | 9E-06 | 7E-06 | 0.0025 |
| Mw_no | | | | | | | | | | | 9E-06 | 9E-06 |
| Md_no | | | | | | | | | | | | 0.3065 |
| Mwd_no | | | | | | | | | | | | |

**Table S5.** Principal components, principal components analysis of population densities of resilient simulations one year prior to perturbation.

| PC | Eigenvalue | % variance explained |
|---|---|---|
| 1 | 1.796 | 44.90 |
| 2 | 1.129 | 28.23 |
| 3 | 0.600 | 15.01 |
| 4 | 0.474 | 11.86 |

**Table S6.** Principal component loadings of populations on first two principal components of analysis of population densities of resilient simulations one year prior to perturbation.

| Population | PC1 | PC2 |
|---|---|---|
| kelp | 0.5513 | -0.3808 |
| understory algae | -0.4123 | 0.6469 |
| sea urchins | 0.4907 | 0.4944 |
| sunflower sea stars | 0.5341 | 0.4383 |

**Table S7.** Chi-square probabilities comparing state frequencies of models with standard consumer mortality rates, and increasing variance of the scaling factor. The Historical and Modern without sea otters models were not tested at the 1% level because they were already consistent at the 5% level.

| **Model** | **1%** | **5%** | **10%** |
|---|---|---|---|
| Historical | – | 0.075 | <0.00001* |
| Historical without sea otters | 0.096 | 0.042* | 0.034* |
| Modern | 0.207 | 0.003* | <0.00001* |
| Modern without sea otters | – | 0.427 | 0.0004* |

## 4.2 Figures

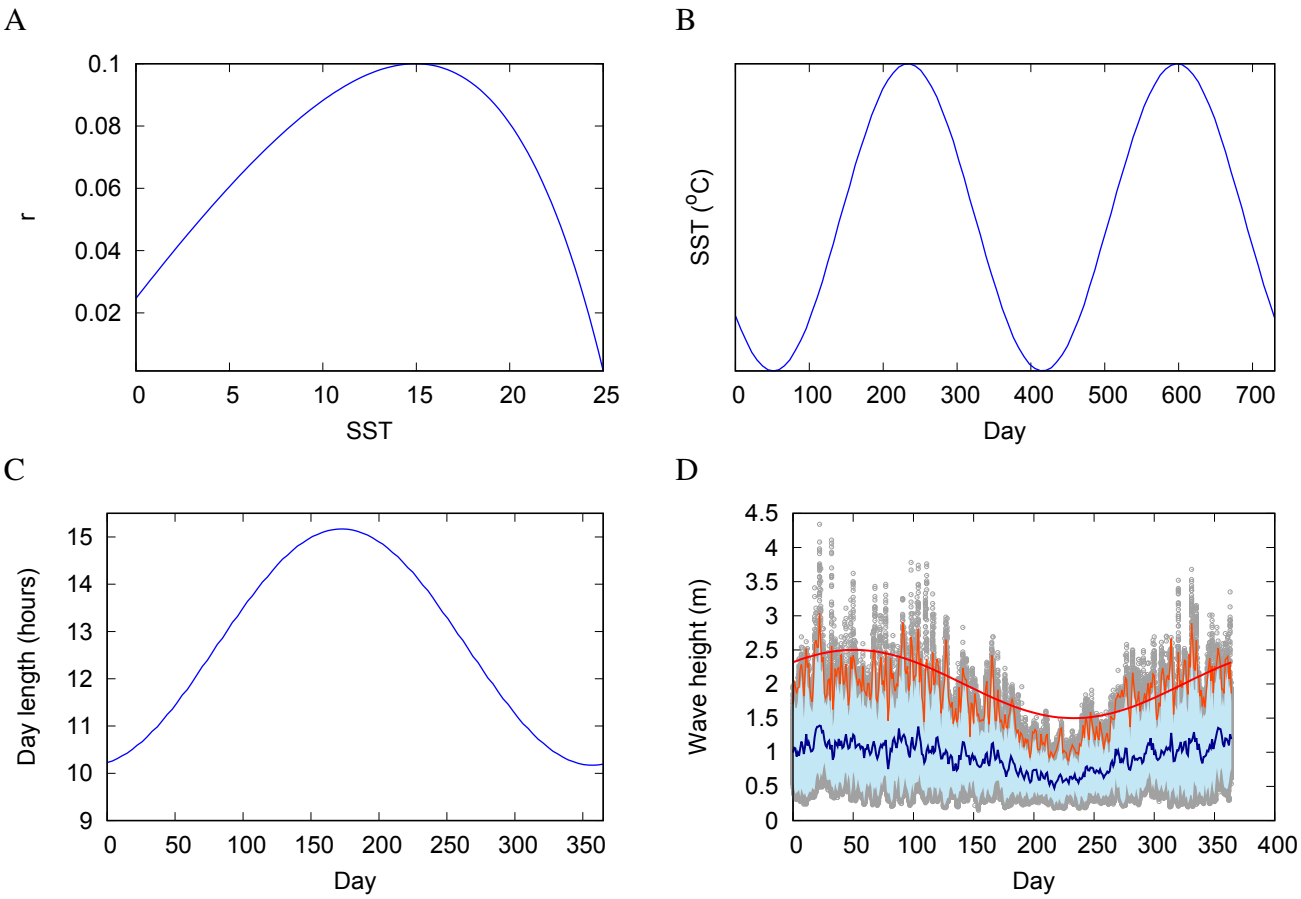


**Figure S1.** (**A**) Relationship between sea surface temperature (SST) and $r$ for the kelp *Macrocystis pyrifera*. $T_{\mathtt{opt}}$ is 15°C. (**B**) Annual SST variation, Monterey Bay. (**C**) Day length, $D$, throughout the year, Monterey Bay. Here $D$ refers to light levels sufficient for photosynthesis to occur within the upper 1.0 m of the water column. (**D**) Annual wave height variation, Monterey Bay, 2009-2020. Grey circles - raw data. Dark blue line - mean. Light blue solid background - 5-95% empirical variation. Light red line - approximate daily maximum during total interval, $2.33\sigma$ above the mean. Solid red line - cosine function estimating daily maxima.

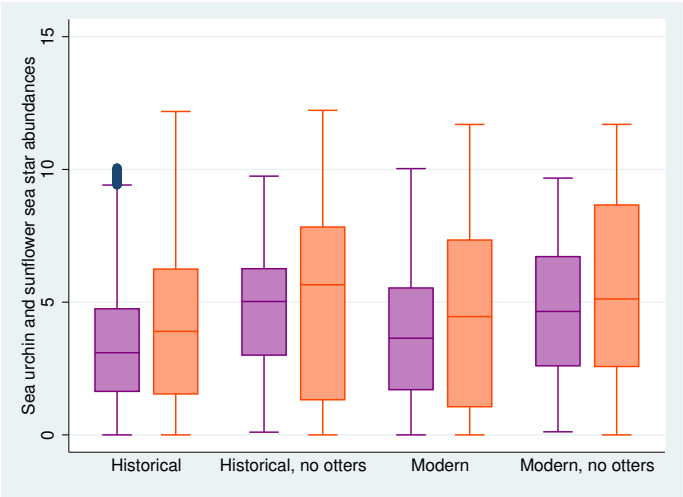


**Figure S2.** Sea urchin and sunflower sea star relative abundances in unperturbed forests. Purple - sea urchins; orange - sunflower sea stars. There are no differences among model types, but abundances are higher when sea otters are absent.

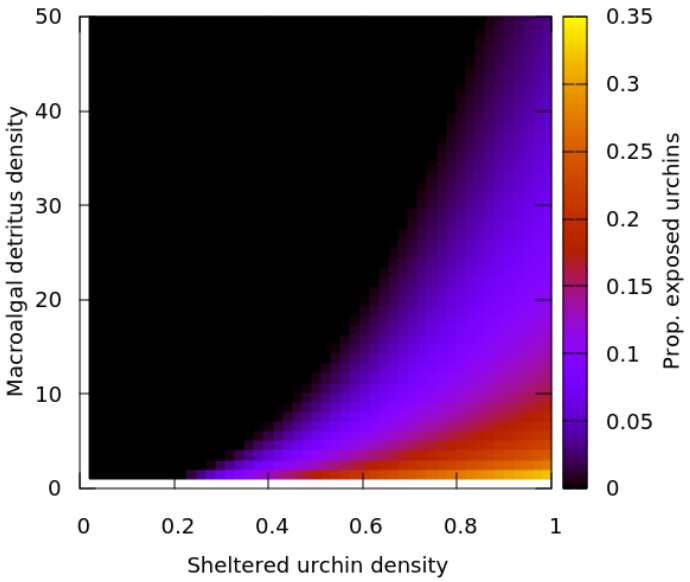


**Figure S3.** The proportion of the urchin population that is exposed ($U_E$), as a function of urchin density and detrital concentration. The colour spectrum scale is shown on the right vertical bar.

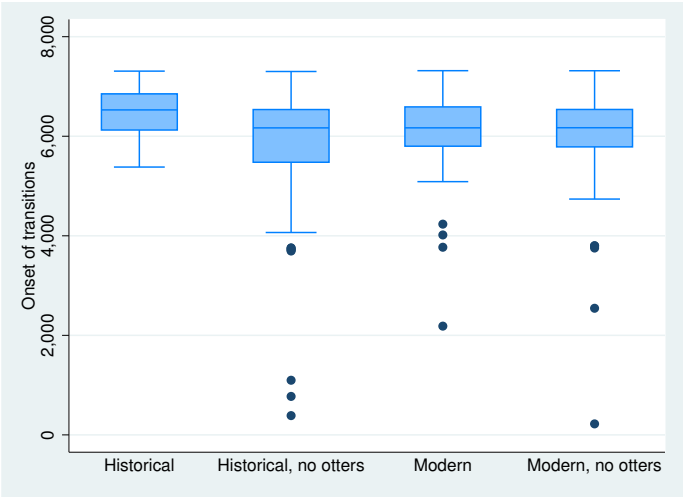


**Figure S4.** Distributions of onset times of transitions after the initiation of perturbation (day 0). SSWD and MHW+SSWD perturbations are pooled within models.

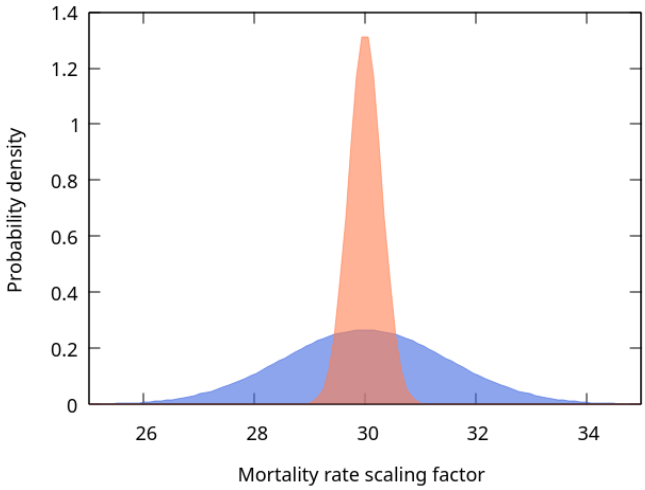


**Figure S5.** Sensitivity distributions of mortality rate scaling factors for *P. helianthoides* and *H. gigas*. Distributions illustrate the variation around $x$ within which sensitivity tests remain consistent with the standard models. Blue - Historical with sea otters, and Modern without sea otters; orange - Historical without sea otters, and Modern with sea otters.